J Neurophysiol 104: 2103–2115, 2010.
First published August 18, 2010; doi:10.1152/jn.00728.2009.

Visuomotor Velocity Transformations for Smooth Pursuit Eye Movements

Gunnar Blohm[1,2] and Philippe Lefèvre[2]

[1]*Centre for Neuroscience Studies, Department of Physiology and Faculty of Arts and Science, Queen's University, Kingston, Ontario, Canada; and* [2]*Centre for Systems Engineering and Applied Mechanics and Institute of Neuroscience, Université Catholique de Louvain, Louvain-la-Neuve, Belgium*

Submitted 10 August 2009; accepted in final form 12 August 2010

Blohm G, Lefèvre P. Visuomotor velocity transformations for smooth pursuit eye movements. *J Neurophysiol* 104: 2103–2115, 2010. First published August 18, 2010; doi:10.1152/jn.00728.2009. Smooth pursuit eye movements are driven by retinal motion signals. These retinal motion signals are converted into motor commands that obey Listing's law (i.e., no accumulation of ocular torsion). The fact that smooth pursuit follows Listing's law is often taken as evidence that no explicit reference frame transformation between the retinal velocity input and the head-centered motor command is required. Such eye-position-dependent reference frame transformations between eye- and head-centered coordinates have been well-described for saccades to *static* targets. Here we suggest that such an eye (and head)-position-dependent reference frame transformation is also required for target *motion* (i.e., *velocity*) driving smooth pursuit eye movements. Therefore we tested smooth pursuit initiation under different three-dimensional eye positions and compared human performance to model simulations. We specifically tested if the ocular rotation axis changed with vertical eye position, if the misalignment of the spatial and retinal axes during oblique fixations was taken into account, and if ocular torsion (due to head roll) was compensated for. If no eye-position-dependent velocity transformation was used, the pursuit initiation should follow the retinal direction, independently of eye position; in contrast, a correct visuomotor velocity transformation would result in spatially correct pursuit initiation. Overall subjects accounted for all three components of the visuomotor velocity transformation, but we did observe differences in the compensatory gains between individual subjects. We concluded that the brain does perform a visuomotor *velocity* transformation but that this transformation was prone to noise and inaccuracies of the internal model.

INTRODUCTION

Smooth pursuit eye movements are generated as a voluntary motor response for tracking moving targets. It is well established that the predominant drive for smooth pursuit initiation is target velocity on the retina (i.e., retinal slip), although target acceleration and position can also have an influence (e.g., Ilg 2008; Ilg and Thier 2008; Krauzlis 2004; Lisberger 2010). Once smooth pursuit has been initiated, afferent visual feedback as well as efference copies of the motor commands are used for pursuit maintenance (Lisberger et al. 1987). The traditional view of how smooth pursuit eye movements are initiated involves computing a two-dimensional (2D) velocity-based motor plan from the retinal slip information, which is then used to drive the 3D ocular plant (Angelaki and Hess 2004; Dicke and Thier 1999; Ghasia et al. 2008; Klier et al. 2006; Tweed et al. 1992). This view proposes that 3D behavioral constraints such as Listing's law, which allows for 2D control of a 3D plant, are implemented through the extraocular muscle-pulley system (Demer 2004, 2006, 2007; Quaia and Optican 1998). Whether Listing's law is indeed implemented through the extraocular muscle-pulley system or rather is actively controlled by neurons in the brain is still under debate (Dimitrova et al. 2003; McClung et al. 2006). Regardless of the answer, this view ignores the fact that the sensory velocity information from the retina must first be interpreted in a geometrically accurate fashion and thus requires a visual-motor transformation of retinal slip to compute a 2D motor plan that moves the eyes in the correct direction. Only once a geometrically accurate 2D motor plan has been established, kinematically correct 3D eye movements that obey Listing's law can be generated.

The need for a visual-motor transformation of velocity signals mainly arises from the eye's ability to rotate around the line of sight, i.e., in torsion. Nonzero torsional states can occur in a number of situations including oblique eye positions (Tweed 1997a), ocular counter-roll during head roll (Bockisch and Haslwanter 2001; Haslwanter et al. 1992), vertical eye positions during head pitch (Bockisch and Haslwanter 2001; Haslwanter et al. 1992), horizontal eye positions during ocular vergence (Mok et al. 1992; Tweed 1997b; Van Rijn and Van den Berg 1993), during the vestibuloocular reflex (VOR) (Bockisch et al. 2003; Harris et al. 2001; Misslisch and Hess 2000) or the optokinetic reflex (OKR) (Fetter et al. 1995; Tweed et al. 1992). This variety of influences results in very different torsional states across viewing situations. Because of these different torsional states, the retinal velocity signals are rotated with respect to the oculomotor apparatus, which in turn is fixed to the skull. This means that to initiate smooth pursuit from a specific visual input, the brain must account for that torsion. Therefore we argue here that an explicit visual-motor transformation of retinal velocity signals is required for spatially accurate smooth pursuit initiation. In other words, the classical 2D motor planning stage must incorporate a transformation of the retinal velocity signals into a reference frame that is independent of the eye's torsional state, e.g., head-centered coordinates.

It is often believed that Listing's law deals with the visual-motor reference frame transformation and renders an explicit transformation unnecessary; however. this is not the case. Listing's law constrains the three degrees of freedom of eye rotation to effectively two axes of rotation that are optimal in the sense that eye velocity is minimal and there is no accumulation of ocular torsion (Tweed et al. 1992). Both types of orienting eye movements, i.e., saccades and smooth pursuit, obey Listing's law (Tweed and Vilis 1990; Tweed et al. 1992). However, Listing's law does not solve the reference frame

Address for reprint requests and other correspondence: G. Blohm, Queen's University, Centre for Neuroscience Studies Botterell Hall 18, Stuart Street, Kingston, Ontario K7L 3N6, Canada (E-mail: Gunnar.Blohm@queensu.ca).

problem; it simply uses a 2D motor plan and ensures that whatever movement is executed, the torsional component of the final 3D eye position is zero (or a specific value specified by a binocular, head-unrestrained version of Listing's law). In addition, as mentioned in the preceding text, some eye movement types do not follow Listing's law, e.g., ocular counter-roll, OKN, or VOR. Therefore Listing's law does not imply any particular reference frame and is merely a constraint on the motor output (or a way for the brain to drive a 3D plant from a 2D motor plan). Consider an example from the saccadic system, where this confusion has essentially been resolved (Crawford et al. 2003). If ocular torsion was 10°, per se (e.g., due to head movements), and a saccade target was displayed, the visual input would be rotated by 10°, relative to the head-centered reference frame—the required motor output reference frame (Crawford and Guitton 1997). If the saccade was programmed in a retinal reference frame (i.e., based only on the position of the target on the retina), we would expect this eye movement to deviate by 10° from the spatial target direction, but the saccadic eye movement would nevertheless conform to Listing's law (no accumulation of torsion). However, we know that for spatially accurate saccades, the retinal input is transformed into a head-centered reference frame (Crawford and Guitton 1997; Hepp et al. 1993; Sparks and Mays 1990). We propose that the same reasoning should also apply to velocity-driven smooth pursuit. Hence in this case, retinal velocity must be interpreted differently depending on 3D eye position signals to generate spatially accurate pursuit.

In the present study, we describe the mathematics of the visuomotor velocity transformation geometry for eye movements without which we expect specific errors in initial smooth pursuit eye movements to occur. We tested three different geometrical constraints in the visuomotor transformation and made specific predictions with respect to each one based on the existence of a specific visuomotor velocity transformation: the axis of eye rotations should change when pursuit is initiated from vertical eye orientations; for oblique eye positions, the visuomotor transformation must correct for the retinal projection geometry, which creates a mismatch between the retinal axes and the projection of the spatial axes onto the retina; and ocular torsion (e.g., due to ocular counter-roll during head roll) should be taken into account. We tested these predictions experimentally and report that the brain compensated for any mismatch between the retinal representation and the required (head-centered) motor output to produce spatially accurate behavior. We discuss the implications of this study for other visuomotor or vision experiments using moving stimuli and make predictions about the underlying neurophysiology.

METHODS

Model

We addressed if and how retinal velocity signals would be transformed into geometrically accurate, smooth pursuit eye movements. Underlying these questions is the fundamental fact that retinal input and extraocular muscle commands are encoded in different frames of reference (see INTRODUCTION). For saccades, it has been shown that position signals must undergo a transformation between the retinal (visual input) and head-centered (motor output) reference frames (Crawford and Guitton 1997). Here we investigated this reference frame transformation for velocity signals.

To do so, we built a geometrical model that transformed visual inputs from a retinal into a head-centered reference frame by taking the 3D eye position into account (see APPENDIX for mathematical details of the model). This was done by constraining 3D eye rotation axes to a 2D surface, as modeled by Listing's law (Tweed 1997a). In its simplest form, Listing's law states that the eyes are in a given position that can be achieved by a single rotation from the "straight-ahead" gaze direction and that the axis of this rotation lies in a fronto-parallel (with respect to the head) plane that passes through the center of the eyes. Implementing Listing's law allowed us to model the effect of vertical eye positions onto the required ocular rotation axis for programming eye movements (APPENDIX, *Eq. A1—A4*). In addition, we allowed for changes in eye torsion, e.g., due to head-roll related ocular counter-roll (APPENDIX, *Eq. A5*) (Bockisch and Haslwanter 2001; Haslwanter et al. 1992), creating a rotation of the visual image with respect the head-centered reference frame (APPENDIX, *Eq. A6*). Finally we implemented the spherical projection geometry of the visual image onto the retina (Blohm and Crawford 2007; Crawford and Guitton 1997), which—together with Listing's law—resulted in the misalignment for the spatial and retinal axes in oblique eye positions. The predictions of this model will be described in more details in RESULTS.

We proposed two extreme working hypotheses that should allow interpreting the experimental data. First, retinal velocity input was used to generate the motor command in an invariable way, i.e., there was no reference frame transformation (retinal hypothesis) or second, retinal velocities are interpreted differently for different eye positions, producing a reference frame transformation (spatial hypothesis). In RESULTS, we first investigated whether hypothesis 1 would lead to errors in the motor command, and how large they would be under different circumstances such as the rotation geometry due to a mismatch between retinal and spatial axes or head roll-induced ocular torsion. (Note: the mismatch of retinospatial axes indicated that for oblique eye positions, the screen vertical did not align with the retinal vertical despite a 0 torsional component in the rotation axis). By design, hypothesis 2 predicted no errors in the generated motor command. We then compared the errors subjects made in initiating smooth pursuit to the predictions from both hypotheses. The experiments (described in the following text) targeted each component of the visuomotor velocity transformation separately.

Subjects

Six human subjects (aged 22–32 yr) were recruited after informed consent. Five of those six subjects were naïve as to the purpose of the experiment. All subjects had normal or corrected-to-normal vision and did not have any known neurological, oculomotor or visual disorders. All procedures complied with the Université Catholique de Louvain Ethics Committee in compliance with the Declaration of Helsinki.

Apparatus

Subjects sat in complete darkness 90 cm in front of a tangent screen. In *experiments 1* and *2,* their heads were restrained by a chin rest, whereas in *experiment 3,* their heads were free to move. Green and red 0.2° laser (BFi Optilas) spots were back-projected onto the translucent screen by means of M2 and M3ST mirror galvanometers (GSI Lumonics, Billerica, LA). Movements of both eyes were recorded at 400 Hz using a Chronos head-mounted 3D video eye tracker (Chronos Vision, Berlin, Germany). The Chronos eye tracker had a tracking resolution better than 0.05° along all three axes. Calibration was accurate to 0.5° in position. Head movements (in *experiment 3*) were recorded at 200 Hz using a Codamotion system (Leicestershire, UK) after placing three active infrared diodes on the Chronos helmet. The arrangement of the Codamotion markers on the eye tracker helmet (see following text) resulted in an estimated resolution (and accuracy) of 0.1° for head movements. Target presentation, position

and velocity commands as well as synchronization signals for eye and head movement recordings were generated at 1 kHz using a dedicated real-time computer (PXI-8186, National Instruments, Austin, TX) running LabView (National Instruments) and PXI-6025E (National Instruments) multi-purpose data acquisition boards.

Procedure

Subjects were presented with a series of blocks of trials. There were three different experiments per session. A calibration sequence consisting of nine fixation positions (0, ±10, and ±20° horizontal and vertical, arranged in the shape of a cross) was presented on the screen before each experiment. Subjects performed two blocks of 50 trials each, per experiment.

EXPERIMENT 1 (EYE ROTATION GEOMETRY). A red fixation spot was presented with a random duration of 750–1,250 ms, at one of three randomly chosen vertical eccentricities, i.e., 0 or ±20° (Fig. 1*A*). After this initial fixation, the target jumped either left or right (±25° horizontal) and immediately started moving either to the left or to the right at 20°/s for 500 ms. The trial ended when the target disappeared. Subjects were instructed to fixate and pursue the target with their head restrained by a chin rest.

EXPERIMENT 2 (RETINAL PROJECTION GEOMETRY—MISMATCH OF RETINO-SPATIAL AXES). Subjects fixated on one of three red fixation spots for a random duration between 750 and 1,250 ms (Fig. 1*B*). The oblique fixation positions were (H, V) (±25, 25) degrees, and we also included a straight-ahead reference position at (0, 0) degrees. Next the target began moving randomly at 20°/s for 500 ms, in one of the four cardinal directions. Subjects were instructed to fixate and pursue the target without moving their head, which was restrained by a chin rest.

EXPERIMENT 3 (HEAD ROLL—TORSIONAL COUNTER-ROLL). Subjects were asked to fixate on a straight-ahead red fixation spot for 1,000 ms (Fig. 1*C*). Then the fixation spot turned green for 750 ms, which indicated to the subjects to tilt (roll) their head, either toward the left or right shoulder. Subjects performed a complete block with head rolls toward the same shoulder and then switched the roll direction in the second block. They were instructed to complete the head roll movement within the 750 ms during which the green fixation spot was presented. After that, the fixation spot turned red again for 250 ms and then began moving at 20°/s for 500 ms in one of the four cardinal directions (randomly selected for each trial). Subjects were required to pursue the target and return to a straight-ahead head position after the target disappeared during the intertrial interval (no target on screen for ~1.5 s). Subjects were free to move their head to any chosen eccentricity; this was a desirable feature that allowed us to obtain a continuum of torsional eye positions, which allowed us to perform regression analysis on the data.

Analysis

The 3D eye-in-head position was extracted off-line from the saved images of the eyes using the Iris software (Chronos Vision). To do so, we used a calibration sequence to calibrate horizontal and vertical eye position as well as to identify the eye ball parameters required for the algorithm to extract ocular torsion (Moore et al. 1996; Peterka and Merfeld 1996). Ocular torsion was obtained from cross-correlation between iris segments across images (Schreiber and Haslwanter 2004), which did not require calibration. Measured eye-in-head position was low-pass filtered (autoregressive forward-backward filter, cutoff frequency = 50 Hz) and differentiated twice (weighted, central difference algorithm, width = 20 ms). Saccades were detected using a 500°/s^2 acceleration threshold, which has been shown to be robust during ongoing smooth pursuit (Blohm et al. 2003; de Brouwer et al. 2001, 2002). Smooth pursuit onset was detected using a velocity backward interpolation technique, as previously done (Badler and Heinen 2006; Carl and Gellman 1987; Krauzlis and Miles 1996). Briefly, we detected the moment after target movement onset at which the absolute eye velocity consistently (i.e., for >50 ms) exceeded 3*SD of the fixation noise (measured before target movement onset) and fitted a regression line on absolute eye velocity over the first 50 ms after this threshold. Pursuit onset was defined as the moment at which this regression line intersected the zero velocity axis. For the analysis, we computed the initial pursuit direction of eye movement and related eye rotation axes, based on the 100 ms open-loop period after movement onset. Data from all random target movement directions were normalized and merged for analysis.

For *experiment 3,* the positions of the three head-mounted infrared markers were low-pass filtered (autoregressive forward-backward filter, cutoff frequency = 50 Hz) and used to calculate the head orientation quaternion. As a reference position for the head, we used the straight-ahead head position measured from the calibration file (where the subject's head was not moving). Head orientation was then computed as the

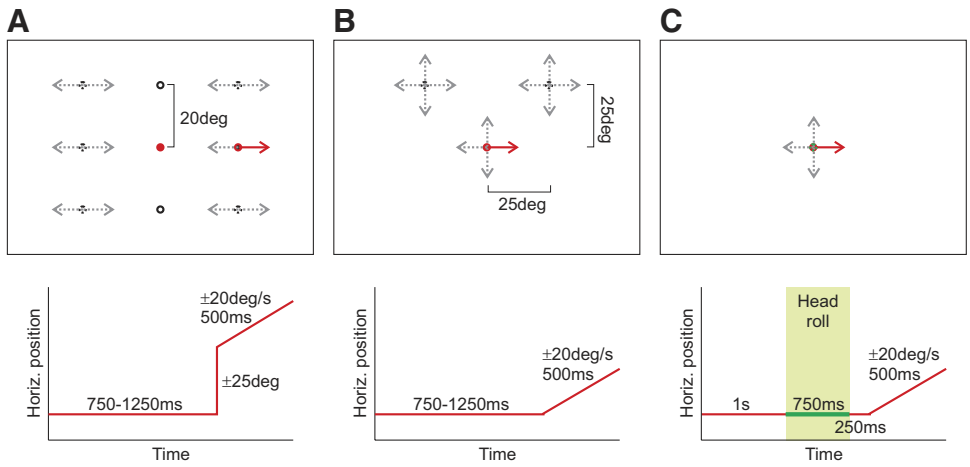

FIG. 1. Paradigms. *A*: test for projection geometry. *Top*: schematic depiction of the spatial arrangement of the stimuli; *bottom*: the time course (horizontal) of the highlighted (red) target motion. Initial fixation (750–1,250 ms) was at 1 of the 3 central vertical positions, 20° apart. Then the target jumped (±25°) and immediately moved for 500 ms at 20°/s either to the left or right. *B*: test for compensation for retino-spatial axes mismatch. The initial fixation target was presented for 750–1,250 ms, either centrally or on the upper oblique lines at positions (H, V) = (±25, 25) degrees. Then targets moved for 500 ms in 1 of the 4 cardinal directions at 20°/s. *C*: torsion due to ocular counter-roll test. After 1 s of fixation on a red, central spot, the fixation target turned green for 750 ms, indicating to the subject to roll his/her head either to the left or to the right (fixed within a block of trials). After an additional 250 ms of red fixation, the target moved for 500 ms at 20°/s in 1 of the 4 cardinal directions.

difference (calculated in terms of quaternion rotation) between this reference position and the measured head position during the test trials.

Eye position traces are presented in Fick coordinates to comply with current literature standards. Positive horizontal and vertical directions are right- and upward, respectively; positive torsion is clockwise.

RESULTS

In each of the following three sections, we first provide quantitative predictions from our model, regarding errors that would be expected in the initial pursuit direction if the geometry between the retinal input (eye-centered) and motor output (head-centered) was not taken into account in the visuomotor velocity transformation. To do so, we analyzed three components of the visuomotor velocity transformation that individually addressed the different geometrical problems the brain faces when transforming velocity signals from a retinal into a motor reference frame. In a second step, we tested each prediction experimentally by measuring the initial direction of smooth pursuit eye movement, as a test of the visuomotor velocity transformation.

Experiment 1: accounting for the rotational geometry of the eyes

The first prediction concerns the rotational geometry of the eyes and is illustrated in Fig. 2. Two different example configurations are shown in Fig. 2*A*, where a horizontal pursuit eye movement was generated in response to a horizontally moving target, viewed under two different vertical eye positions, i.e., a central eye position (dotted, green) and a 20° upward eye position (solid red lines). The circular representations in the two panels to the right of the subject's head show that both situations result in exactly the same retinal input: the moving target presented on the retinal horizon, thus the retinal velocity input was purely horizontal. In general, all points on a vertically offset horizon, passing through a fixation position on a fronto-parallel surface, projected onto the retinal horizon if ocular torsion and head roll angles were zero (as was the case here). However, the motor output required for spatially accurate pursuit depended on vertical eye position. The angular velocity axis for pursuit initiation under straight-ahead viewing was purely vertical (dotted green lines), whereas pursuit initiation during nonzero vertical fixation required an angular velocity axis that was tilted by half the amount of vertical eye position (solid red lines), as predicted by ½-angle rule (Tweed and Vilis 1987). This meant that for the visuomotor velocity transformation, the brain should account for vertical eye position when interpreting identical visual input, thus generating spatially accurate pursuit initiation. Although we restricted ourselves to the vertical eye position, the same principles apply when generating vertical pursuit from different horizontal fixations.

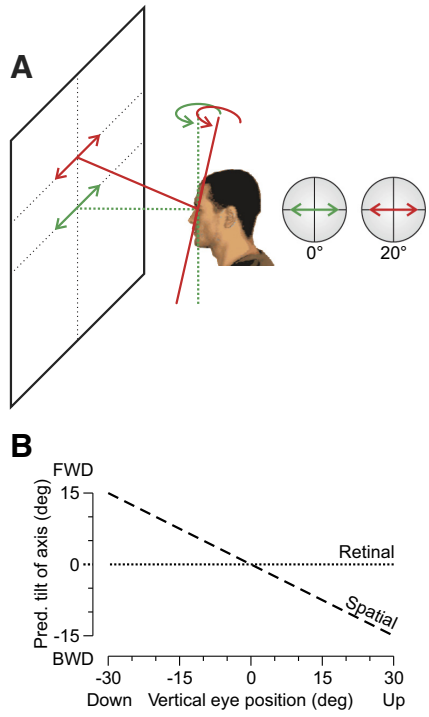

FIG. 2. Effect of the retinal projection geometry on the visuomotor velocity transformation. *A*: the same retinal stimulation (*left*) led to different head-centered motor commands (*right*). For straight-ahead fixation (dotted green), a target moving to the right (arrow) required a purely horizontal eye movement (rotation around the vertical axis, *right*). For an eye-elevation of 20° (solid red line), the same retinal stimulation must be transformed into a different eye rotation with a nonvertical rotation axis, following the ½-angle rule. *B*: predicted rotation of the velocity vector, if the brain takes vertical eye position into account and interprets the retinal stimulation differently for different eye positions (dashed, spatial hypothesis) or interprets the visual input independently of eye position (dotted, retinal hypothesis).

Figure 2*B* illustrates the degree of predicted tilt of the angular eye velocity axis required for accurate pursuit initiation as a function of the initial vertical fixation position. Thus the tilt of the rotation axis results in a torsional component of the 3D rotation axis. In other words, the velocity command driving the eyes must move the eyes by the amount of torsion specified by the torsional component of the rotation axis so as to maintain Listing's law. For spatially accurate, smooth pursuit initiation (*hypothesis 2*), the angular velocity axis has to tilt back by half of vertical eye position. In contrast, *hypothesis 1* (retinal model) would predict no change in the rotation axis with vertical eye position. An example of the spatially accurate behavior was observed in our typical trial, and is shown in Fig. 3.

Figure 3*A, top,* shows a plot of 3D eye position (horizontal, vertical, and torsion) in response to the target, over time; *A, bottom,* depicts eye velocity over the same period. Initial fixation was on the upward target with a 20° elevation; the target then jumped to the right and moved leftward. The vertical dotted line indicates when the pursuit target began to move and the vertical solid line (Fig. 3*A, bottom*) represents the detected onset of pursuit eye movement, which occurred around 125 ms after the target started moving. Note that smooth pursuit was initiated prior to the catch-up saccade when the eyes were still at approximately zero horizontal position. Therefore the initial pursuit response relied fully on sensory evidence in the visual periphery that was gathered during fixation on the vertical mid-line (unlike the situation described in *experiment 2*). We computed the eye rotation axis from the first 100 ms of pursuit (i.e., during the open-loop pursuit phase). The rotation axis ω can easily be computed using (Tweed and Vilis 1987)

$$\omega = 2 \cdot \dot{q} q^{-1}$$

where $\dot{q}$ is the mean quaternion velocity computed over the first 100 ms after pursuit onset and q^{-1} is the quaternion inverse of the

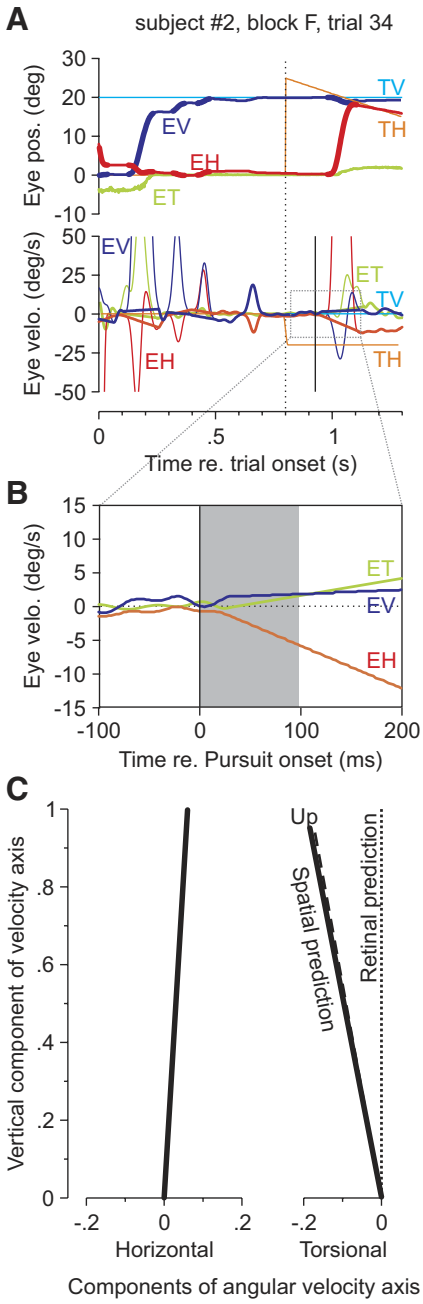

FIG. 3. Typical rotation geometry trial. *A*: position in degrees (*top*) and velocity in degree/second (*bottom*) traces over time. Horizontal eye (red solid, saccades bold) and target (orange) traces, vertical eye (blue) and target (light blue) traces and torsional eye position (green) are shown (*top*). The same color scheme applies for the *bottom* (velocity), but now saccades are thin traces (pursuit velocity without saccades is thick). In this trial, initial fixation was 20° up and then the target jumped rightward and moved to the left. The jump/movement onset time is indicated by the dotted vertical line. The solid vertical line in the *bottom* shows detected pursuit onset (latency = 128 ms). All traces use Fick coordinates. *B*: zoom on the eye velocity traces during pursuit initiation. *C*: from the 1st 100 ms after pursuit onset, we computed the angular velocity axis of the eyes (solid line). This axis tilted backward for upward eye positions, as predicted by the spatial hypothesis (dashed) and did not follow the retinal hypothesis (dotted).

average eye position during that same period. Alternatively, we also used the quaternion division of the eye position quaternion at 100 ms after pursuit onset divided by the quaternion at pursuit onset and obtained qualitatively the same results. Figure 3*C* shows that this axis (solid line) followed the spatially correct behavior (dashed line) and did not overlap with the retinal prediction (dotted line).

We quantified the eye position dependence of the angular ocular velocity axis during pursuit initiation across all trials. The result of this analysis is shown in Fig. 4. *A* depicts the three components for the angular velocity axes for data from all subjects pooled together, i.e., the vertical versus horizontal components (*left*) and the vertical versus torsional components (*right*). Again the retinal hypothesis predicted no tilt in the angular velocity axis with vertical eye position, whereas the spatial hypothesis predicted a tilt in the torsional direction (dashed lines). As was observed, the data were close to the spatial prediction and thus pursuit initiation was geometrically accurate. In Fig. 4*B*, we also quantified the amount of tilt in the angular velocity axis for each individual subject by calculating the "tilt gain," relative to vertical eye position. All subjects showed tilts that were significantly different from the retinal hypothesis (*t*-test, $P < 0.001$) and did not significantly differ from the spatial hypothesis (*t*-test, $P > 0.05$). This confirmed previous results (e.g., Tweed et al. 1992) demonstrating that subjects adjusted their rotation axis, depending on the current eye position (see DISCUSSION).

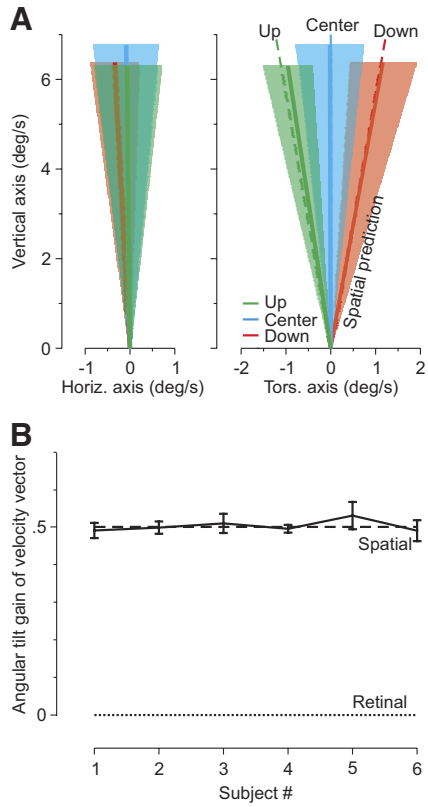

FIG. 4. Tilt of angular velocity axis in the geometry condition. *A*: mean ± SD of the angular velocity axes during pursuit onset for upward (green) central (blue) and downward (red) initial eye position. The predictions of the spatial hypothesis for the upward and downward fixations are also shown (dashed). *B*: tilt gain of angular velocity vector (mean ± SE). Dashed and dotted lines depict the spatial (½-angle rule) and retinal hypotheses, respectively. All subjects showed tilts close to the spatial prediction (dashed) that significantly differed (*t*-test, $P < 0.001$) from the retinal prediction (dotted).

Experiment 2: effects of retinal projection geometry (mismatch between retinal and spatial axes)

The second prediction of our model addressed the misalignment between the retinal and spatial axes for oblique eye positions. This misalignment occurred even when the head was restrained and was due to the rotational geometry of the eyes and the spherical projection geometry. It can also be affected by small torsional changes related to each individual subject's Listing's law.

Figure 5 depicts the consequences of the purely geometrical component (mismatch of retino-spatial axes) on the retinal projection for oblique eye positions. Targets moving along the cardinal axes on the screen (*A, left*) project onto the retina (right circular representation) in different manners, depending on eye-in-head position (*bottom*: views of the eye from behind). For straight-ahead fixation (green, dashed), the retinal and spatial axes align. However, for oblique positions, for example when fixating up and to the left (solid blue), Listing's law dictates that the eyes are rotated in such a way that the retinal axes tilt, relative to the spatial axes, which is a direct consequence of zero torsional eye rotations (see APPENDIX, *Eqs. A1–A4*). This was also observed from the back view of the eye (lower part of panel), where the retinal axes for a 45° oblique eye position appeared tilted. When measuring eye movements using Euler angles, such tilts result in an apparent torsional component that has been labeled "false torsion," a now outdated concept. As a result, targets moving along the cardinal directions on the screen projected in a rotated fashion onto the retina. This projection pattern was similar for the up-right fixation position (red). This rotation depended on fixation eccentricity along the cardinal axes and is shown in Fig. 5*B* for fixations on the oblique axes in the upper quadrants of the screen. The retinal hypothesis predicted that the brain should not rotate the retinal velocity vector into a spatially congruent representation, whereas the spatial hypothesis predicted that retinal velocity signals should rotate in a spatially accurate representation. Despite this rotation of the visual input on the retina for oblique eye positions, the same spatial pursuit direction should ideally be generated across all fixation positions. Therefore the brain should rotate the visual velocity input, to produce spatially accurate pursuit initiation. This was different from *experiment 1,* where the rotation axes were adjusted as a result of the required 3D motor command that directed the eyes. Here it was the visual input that was rotated as a result of the current 3D eye position.

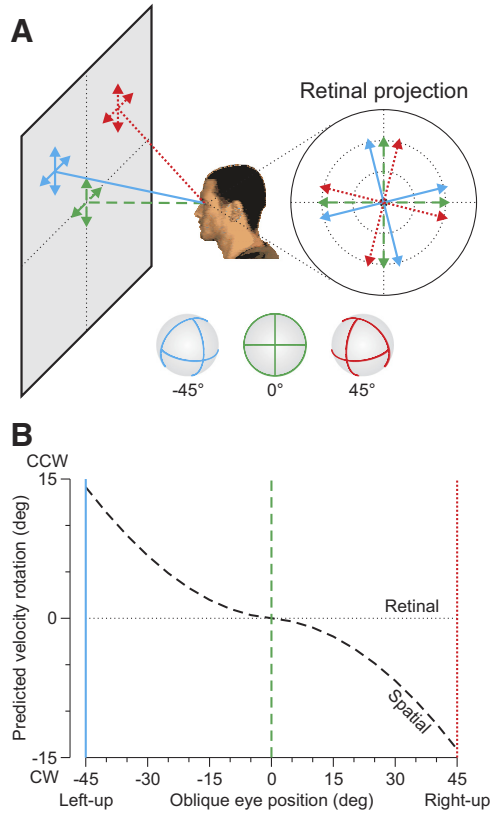

FIG. 5. Mismatch of retino-spatial axes due to oblique orbital positions. *A*: the same 4 cardinal velocity directions (arrows on left side) in head-centered coordinates viewed under different oblique eye positions projected differently onto the retina (right side, flattened retinal map). For straight-ahead fixation (0°, green dashed), the 4 velocity directions projected onto the retinal cardinal axes. At −45° oblique fixation (solid blue), the retinal projection of the velocity vectors was rotated counter-clockwise by about 14°. At 45° oblique fixation (red dotted), the velocity vectors were rotated 14° clockwise on the retina. The brain generated the same head-centered motor command from all three sensory inputs. In the lower part of the panel, we show the 3 different orientations of the eye and retinal cardinal axes in space. *B*: prediction of the velocity vector rotation, as a function of oblique eye position, if the brain did not take mismatch of retino-spatial axes into account, but instead used the retinal velocity vector to generate a motor command. The spatial (dashed black) and retinal (dotted black) hypotheses are shown together with the predictions from *A,* left-up fixation (blue solid line), center fixation (green dashed line) and right-up fixation (red dotted line).

Figure 6 depicts a typical trial demonstrating this behavior. After an initial fixation on a target in the upper left region (Fig. 6*A*), the target started moving to the right. Smooth pursuit initiation (onset delimited by vertical solid line in *bottom*) occurred shortly after target movement onset (delimited by vertical dotted line). Figure 6*B* shows a zoom of the pursuit initiation period and illustrates the spatially accurate behavior. Figure 6*C* shows the 2D direction of pursuit initiation (black dots) for the first 100 ms of the pursuit response to the target movement, i.e., the open-loop period. Comparing this pursuit response to the predictions of spatially accurate behavior (solid dark green) and the retinal hypothesis (dotted light green) suggests that the pursuit system accounted for the mismatch between retino-spatial axes when generating a motor command from visual input.

This observation was analyzed in detail, and all data recorded for this condition are shown in Fig. 7. Figure 7*A* shows the average velocity traces pooled for all subjects for rightward movements, starting from different initial fixation positions, either 25° up and to the left (*top*), straight-ahead (*middle*), or 25° up and to the right (*bottom*). The measured velocity traces in spatial coordinates (solid green, with torsion compensation) and the reconstructed (based on the 3D eye-in-head position) velocity traces in retinal coordinates (dashed red, without torsion compensation) are shown. Spatially optimal behavior is indicated by the dashed horizontal black lines. On average subjects showed clear, spatially optimal behavior.

This behavior was further quantified in Fig. 7*B*, where we performed a regression analysis on the raw data to determine the amount of the predicted compensation for rotation between the retino-spatial axes that was actually observed in the data. Predicted compensation was the rotation theoretically calculated by our model for a spatially accurate pursuit given the measured 3D eye position. Observed compensa-

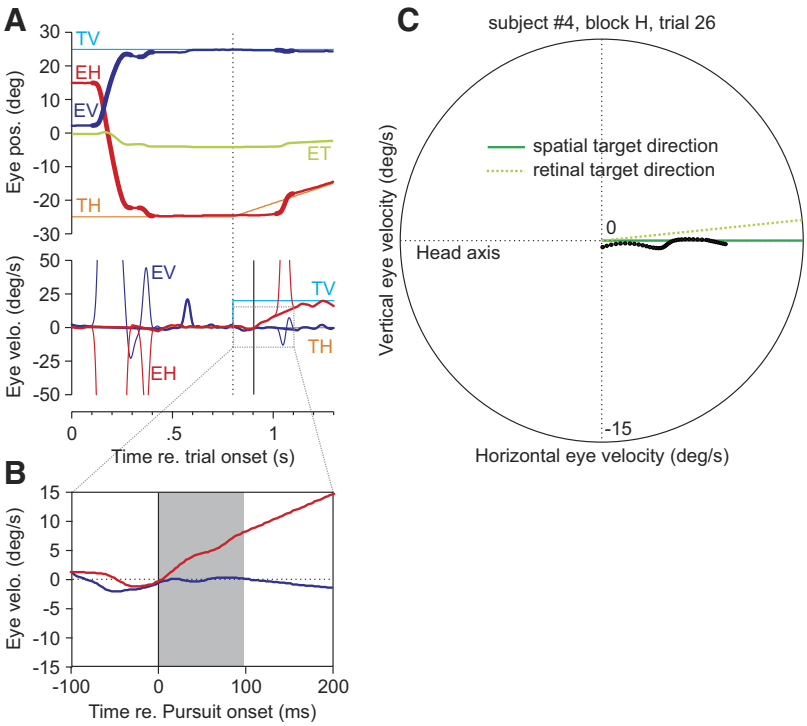

FIG. 6. Typical mismatch of retino-spatial axes trial. *A*: initial fixation was up and to the left, and pursuit direction was rightward. Representation similar to Fig. 3. *B*: zoom on the eye velocity traces during pursuit initiation. *C*: 2D representation of the evolution of eye velocity (black dots), over time and viewed in head-fixed (spatial) axes. Each individual black dot is spaced by 2.5 ms. Eye velocity followed the spatially accurate prediction (solid dark green) and not the retinal prediction (light dotted green).

tion was predicted compensation – (minus) eye velocity direction (re. target direction) in space. The rotation of the retinal image on the retina is variable and depends on the amount of actual torsion (which has some variability), thus the nine arbitrarily chosen bins. The regression slope for data pooled across all subjects was undistinguishable from unity ($P < 0.001$). The compensatory gain in the retino-spatial axis rotation for individual subjects (Fig. 7*C*) indicated that most subjects (all but *subject 5*) had, on average, close to perfect behavior ($P < 0.05$). This confirmed that the pursuit system accounted for the misalignment between the sensory and motor coordinates due to the rotation between the retino-spatial axes.

Experiment 3: compensation for ocular torsion induced by head roll

In this third and final test, we assessed whether actively generated ocular torsion was also accounted for in pursuit initiation. To determine this, we asked subjects to perform fast head roll movements and took advantage of the OCR to obtain a purely torsional misalignment between the retinal input and the motor output required for spatially accurate behavior. The principle of this experiment and the related predictions are illustrated in Fig. 8. Figure 8*A* depicts the counter-roll of the eyes (by an arbitrary amount here) when the head rolls toward the right or the left shoulder. Consequently, the retinal stimulation for the same required eye movement changed across head positions because the eyes were rotated torsionally (because of OCR), relative to the head. Figure 8*B* shows the necessary counter-rotation of the visual input by the brain to compensate for OCR-induced torsion (for illustration purposes, we chose an OCR gain of 0.5). As can be observed from *Eq. A5*, this relationship is linear with head roll angle.

The typical trial in Fig. 9 shows an example of behavior during this condition. The representation in Fig. 9*A* is similar to Figs. 3 and 6 but now includes head position traces (*bottom*). During the head roll instruction (gray rectangle), the subject rotated the head toward the right shoulder; this made the eyes counter-roll in the direction opposite to the head (*top*, green trace). This resulted in a misalignment of the retinal and motor coordinates. Shortly after the head was stabilized (2nd vertical dashed bar shows head movement end), the target started moving (dotted vertical line). Figure 9*B* shows a zoom of the pursuit initiation period and illustrates the spatially accurate behavior. We again examined the first 100 ms of pursuit initiation and plotted pursuit direction as head-centered coordinates (Fig. 9*C*). The target now moved along the spatial direction (solid dark green), and we show the reconstructed retinal target movement direction (dotted light green) for comparison. Clearly, pursuit initiation (black dots) overall followed the spatially correct direction.

Spatially accurate pursuit initiation indicated that the brain actually rotated the retinal velocity vector by the amount of ocular torsion. To quantify this effect, we showed average eye velocity initiation traces (solid green) in Fig. 10*A* for leftward (CCW) and rightward (CW) head roll. We also showed reconstructions of what the velocity traces should look like if OCR-induced torsion was not taken into account (dotted red line); we found that eye velocity followed the spatially accurate direction (dashed horizontal lines). The regression analysis shown in Fig. 10*B* confirmed this observation. The observed torsional compensation closely matched the predicted compensation and the regression slope was not distinguishable from unity (*t*-test, $P < 0.001$). This was also true for most individual subjects (*subjects 1–4*, $P < 0.05$) as shown in Fig. 10*C*. Overall, this demonstrates that the pursuit system actively accounted for ocular torsion when generating a motor plan.

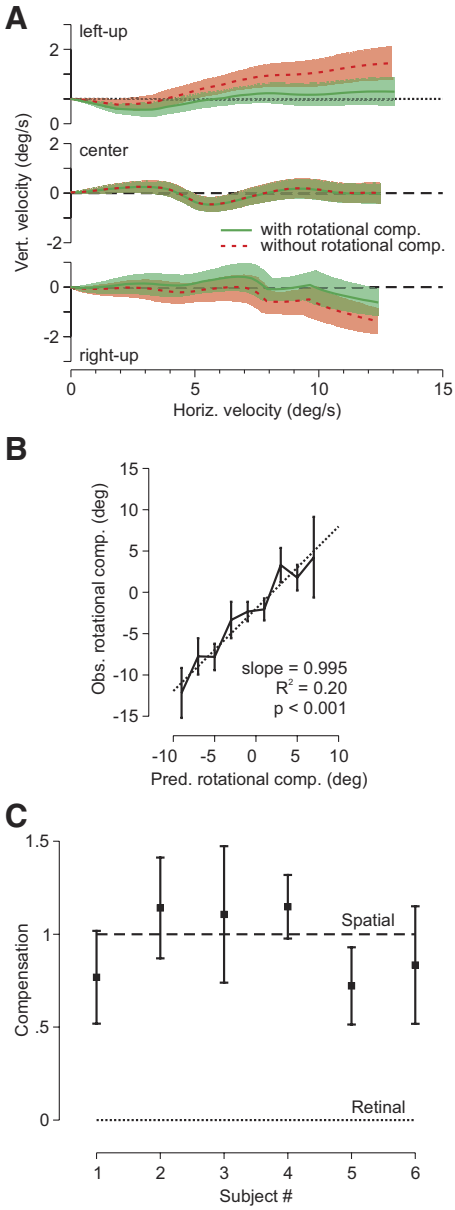

FIG. 7. Compensation for mismatch of retino-spatial axes. *A*: average 2D velocity traces for rightward target movements in the upper left, center, and upper right initial fixation conditions. Measured traces with hypothetical rotational compensation (spatial, solid green), and traces rotated to simulate no rotational compensation (retinal, dashed red) are shown (mean ± SE). Spatially correct behavior would be along the horizontal direction (black dashed line). *B*: observed compensation for the rotation between the retino-spatial axes measured from initial pursuit direction and as a function of the theoretically required (predicted) compensation. The regression line on raw data were not distinguishable from the slope = 1 (*t*-test, $P < 0.001$). *C*: compensation gain (= slope of regression) of the rotation between the retino-spatial axes for individual subjects (mean ± SE). Dashed and dotted lines depict the spatial and retinal hypotheses, respectively. All gains were different from 0 ($P < 0.001$) and all (but *subject 5*) had gains indistinguishable from 1 ($P < 0.05$).

Influence of saccades on pursuit initiation

To quantify the influence of catch-up saccades on our findings, we analyzed the relative latencies of smooth pursuit initiation and catch-up saccades across all trials and conditions in Fig. 11. As can be observed, on average smooth pursuit was initiated almost 100 ms before catch-up saccades were produced (median = 89 ms). This finding was consistent across all three experimental conditions (medians = 85–97 ms). It also means that for about half of all trials, saccades did not have any influence on the measure of the first 100 ms of pursuit initiation, which was the period of interest throughout our analysis. To confirm that velocity interpolation during saccades did not alter our findings, we performed the analysis of Figs. 4, 7, and 10 on a subset of our data without any saccades during the first 100 ms of pursuit initiation and found qualitatively the same results (data not shown). This demonstrates that neither our method of saccade removal nor the presence of saccades during pursuit initiation influences the visuomotor velocity transformations described here.

DISCUSSION

We have developed a model for the visuomotor velocity transformations underlying eye movements. This model made quantitative predictions regarding the movement errors that should occur if the 3D eye-in-head geometry was not taken into account when generating a smooth pursuit eye movement from visual motion input. We tested these predictions using the open-loop smooth pursuit response to moving targets. Our results demonstrated that subjects used eye position in their adjustment of the rotation axis of the eyes. Rotation between the retino-spatial axes was also accounted for, and that ocular torsion due induced by head roll was compensated for when generating a smooth pursuit motor plan. This study provides the first evidence of a feed-forward visuomotor velocity transformation in the brain.

General discussion

On average, our data showed that the brain accurately used extraretinal eye position information to transform the retinal, eye-centered velocity signals into a motor command, specified in head-centered coordinates. However, we observed individ-

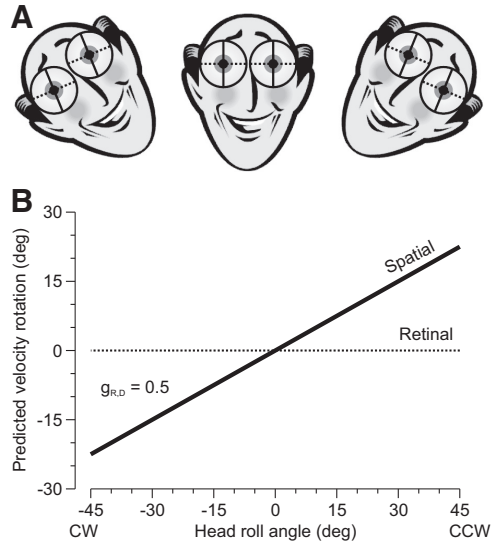

FIG. 8. Effect of ocular torsion (due to ocular counter-roll) on the visuomotor velocity transformation. *A*: schematic representation of ocular counter-roll. For example, if the head rolled 40° to the left, the eyes counter-rolled in the head (by 20°, corresponding to an OCR gain of 0.5). *B*: predicted pursuit velocity rotation, if ocular torsion was (spatial hypothesis, dashed) or was not (retinal hypothesis, dotted) accounted for when generating a motor command from the retinal input.

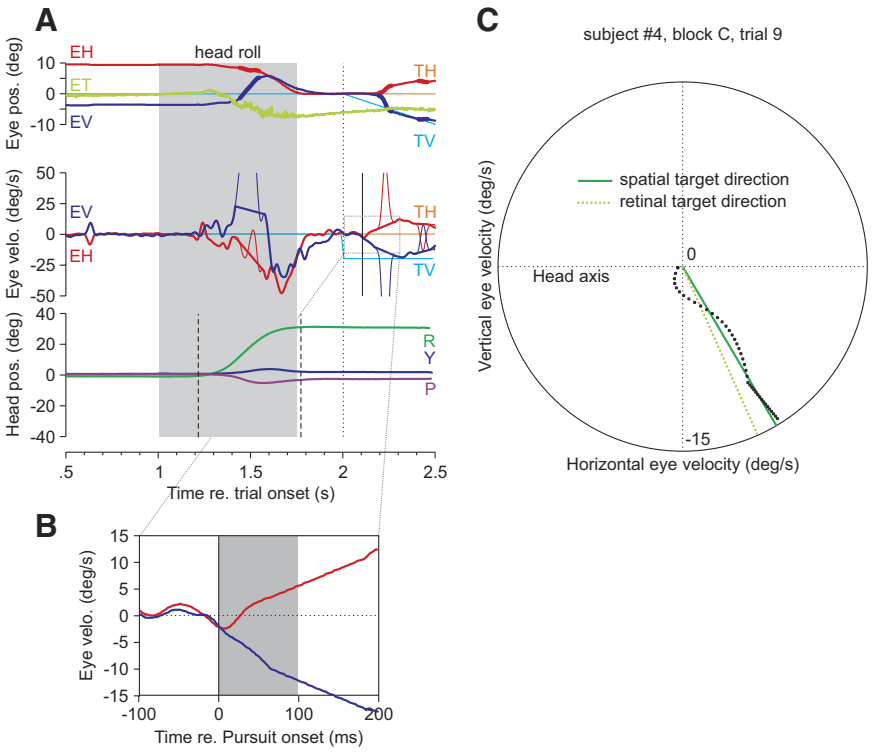

FIG. 9. Typical head roll trial. *A*: same representation as in Figs. 3 and 6 but with additional head position traces (*bottom*). Head pitch (up and down movement, P, purple), head yaw (left to right movement, Y, dark blue) and head roll movements (rotation toward shoulders, R, green) are shown. Gray area shows when the head roll instructions were illuminated (fixation target green). Vertical dashed lines indicate head movement on- and offset (100°/s^2 threshold). The head roll induced an ocular counter-roll movement (see torsional eye position in first panel). This resulted in a misalignment between the retinal input and the required motor output (relative to the head). *B*: zoom on the eye velocity traces during pursuit initiation. *C*: same representation as in Fig. 6*B*. Due to the head roll position, the spatial movement direction was not tilted with respect to the head axes (circle, black dotted lines). Eye velocity (back dots, 2.5 ms spacing) followed the spatial (solid, dark green) and not the retinal (dotted, light green) movement direction of the target.

ual differences in the gain of compensation between subjects. The fact that every subject did not perfectly compensate for the underlying geometrical constraints is likely a consequence of the complexity of these computations and the difficulty with which the brain achieved them. It might also be that the required 3D eye position signal was difficult for the brain to estimate. This is particularly true for ocular torsion. There is no evidence supporting that the cortex has access to an explicit ocular torsion signal (Banks et al. 2001; Schreiber et al. 2001; van Ee and van Dam 2003). Therefore the brain might have to estimate ocular torsion from horizontal and vertical eye position, as well as 3D head position information, making use of an internal model of Listing's law (Blohm et al. 2008b). Of course, this feed-forward visuomotor velocity transformation only has to produce a rough estimate of the spatially accurate movement direction. After pursuit initiation, on-line visual feedback can be used to correct for any errors in the visuomotor transformation.

Previous studies have suggested that the brain might not perform explicit visuomotor transformations for eye movements at all, but that the extraocular muscle properties could account for the observed effects through the use of pulleys (Demer 2006, 2007). In theory, at least part of the visuomotor velocity transformation for eye movements could be implemented mechanically, such as by the half-angle rule (Klier et al. 2006). However, if only passive pulleys were used, they could not account for the compensation of torsion due to ocular counter-roll in our head roll experiment because an explicit visuomotor velocity transformation was required. The brain needs to use extraretinal signals about the torsional state of the eyes (Tian et al. 2007) to counter-rotate the visual input, thus obtaining a geometrically correct motor command in head-fixed coordinates. The same reasoning applies to the situation of retino-spatial misalignment during oblique eye positions. Active pulleys could implement the visuomotor velocity conversion, but the brain would still need to perform the correct 3D computations to send adequate neural commands to the pulleys.

The described rotational properties of the eyes have previously been reported in 3D ocular kinematics (Listing's law). It is well known that the rotation axis for geometrically accurate pursuit in nonzero vertical eye positions has to be tilted. In the velocity description of Listing's rotation vector, this is known as the half-angle rule (Adeyemo and Angelaki 2005; Bruno and Van den Berg 1997; Crawford and Vilis 1991; Tweed and Vilis 1990). As we demonstrated, this problem can also be viewed as a visuomotor velocity transformation problem, especially when considering velocity-driven smooth pursuit eye movements. The retinal input must be adequately transformed into a spatially accurate motor command for the eyes.

There has been a long-standing interest in investigating whether smooth pursuit initiation is governed by retinal or nonretinal representations of target motion (e.g., Chowdhury et al. 2009; Dicke and Thier 1999; Ilg et al. 2004; Inaba et al. 2007; Krauzlis and Lisberger 1989; Lisberger 2010; Lisberger et al. 1987; Pack et al. 2001; Robinson 1965; Wertheim 1981). In other words, does pursuit initiation only depend on retinal slip estimation (retinal representation) that is updated on the flight using new sensory information or does the brain use efference signals of eye velocity to compute instantaneous estimates of target motion in space (world-centered representation). This problem focuses on the question whether extraretinal eye (and head) *velocity* signals are integrated with retinal velocity signals for pursuit initiation, which is very different from the question addressed in the present study, i.e., whether eye (and head) *position* signals are integrated with retinal slip to

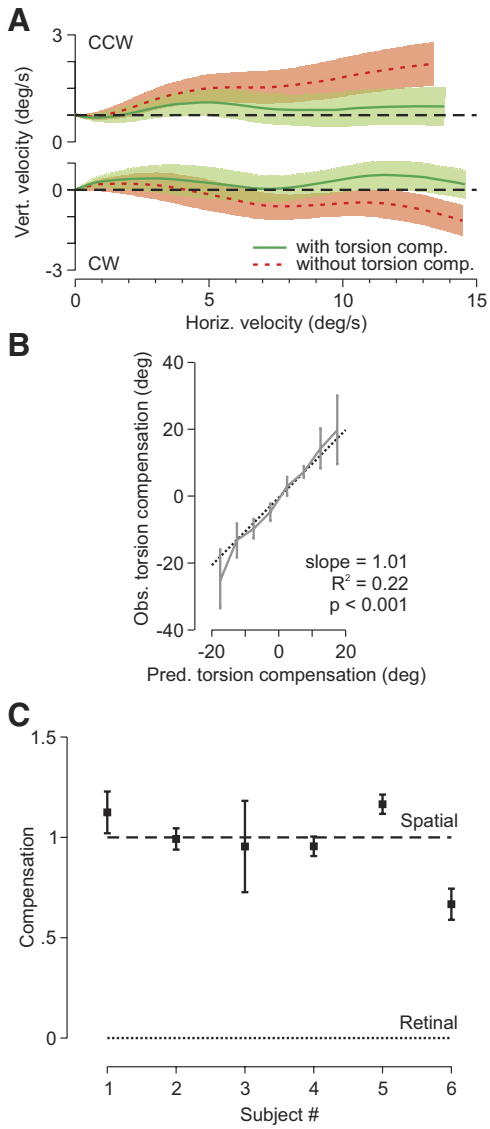

FIG. 10. Compensation for ocular counter-roll (OCR) induced torsion. *A*: similar representation as in Fig. 7*A*. Average directions of pursuit initiation (solid green) and the rotated pursuit direction were measured as if OCR-induced torsion was not taken into account (retinal hypothesis, dotted red). Pursuit direction was normalized to account for head roll. Spatially accurate behavior should therefore follow the horizontal dashed line. *B*: observed compensation for OCR-induced torsion as a function of the compensation required for spatially accurate behavior (predicted). The predicted torsional compensation was approximately equal to the measured ocular torsion. The observed compensation was computed as the difference between the theoretical movement direction without torsion compensation and the measured direction of pursuit initiation. The slope of the regression line on raw data were not distinguishable from 1 (*t*-test, $P < 0.001$). *C*: torsional compensation gains (regression slopes) for individual subjects (means ± SE). Dashed and dotted lines depict the spatial and retinal hypotheses, respectively. All gains were significantly different from 0 ($P < 0.001$) and gains from 4 subjects (*1–4*) were indistinguishable from 1 ($P < 0.05$).

get the geometry of the visuomotor velocity transformation right. The need for a correct geometric transformation is independent of whether the pursuit system uses a retinal or nonretinal representation of target motion and is required in both cases. In the present study, we describe a new, additional geometric transformation that has to be considered when using retinal velocity signals for motor control.

Theoretical considerations

The presence of an explicit visuomotor velocity transformation raises the question of the required neural signals and computations. Retinal target velocity should rotate, depending on ocular torsion; this could be reconstructed based on an internal model of 3D eye position (Blohm et al. 2008b). In addition, horizontal and vertical eye orientation is also needed to compensate for the rotation between the retino-spatial axes and to account for the tilt of the angular velocity axis for eye movements from noncentral eye positions. These signals need to converge to the same brain area that carries out the required calculations. These geometrical computations are relatively complicated for two reasons. *1*) The 3D rotational geometry is nonlinear and noncommutative and is influenced by many different factors (horizontal and vertical eye position, ocular torsion induced by head roll, retinal velocity, and retinal position). *2*) In this process, multimodal signals with different physical meanings (e.g., position vs. velocity) should be thoughtfully combined across different representations (e.g., retinal map vs. distributed eye position code). Although some general theoretical suggestions exist (Deneve et al. 2001), the mechanisms by which the brain performs such computations remain largely unknown. It is also unclear what neural properties would arise in the relevant areas.

Hypothetical underlying neurophysiology

The visuomotor velocity transformation could theoretically be implemented anywhere between V1 and the extraocular muscles. It is even possible that different aspects of this transformation are implemented differently in the brain and/or eye mechanics. However, analogous to parietal areas involved in the visuomotor transformation of *positional* signals (Battaglia-Mayer et al. 2003; Blohm et al. 2008a; Crawford et al. 2004; Optican 2005; Snyder 2000), we suggest an involvement of temporal area MST in the visuomotor *velocity* transformation.

It has been suggested that MST is the temporal area of pursuit (Dursteler and Wurtz 1988; Lisberger 2010), an important area for smooth pursuit initiation and maintenance (for reviews, see Andersen 1997; Krauzlis 2004; Lisberger 2010) at

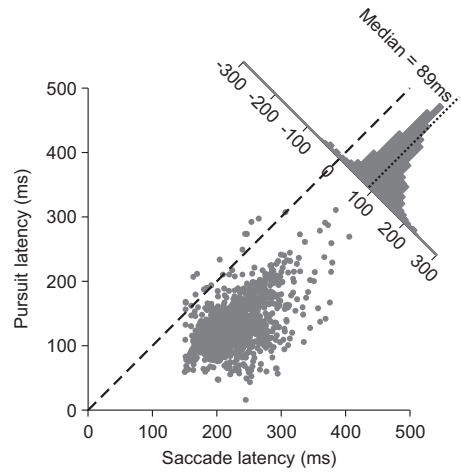

FIG. 11. Relative latencies of smooth pursuit and catch-up saccades. Individual data points represent trials across all 3 conditions. The median of the saccade re. pursuit lag (histogram *inset*) was 89 ms.

the interface between early visual areas and oculomotor areas. Therefore its location makes it an ideal candidate to implement a geometric transformation between a retinal and head-centered reference frame. Theoretically required ingredients for area MST to potentially carry out the reference frame transformation are eye position gain fields, knowledge about ocular torsion (likely through an internal model of 3D eye position, see DISCUSSION in the preceding text), extraretinal eye (and head) velocity signals, and target position signals (in addition to velocity tuning). To our best knowledge, MST meets all these criteria. The last criterion is automatically met through the characteristic combined position-velocity tuning of MST cells (Celebrini and Newsome 1994; Chukoskie and Movshon 2009; Churchland and Lisberger 2005; Komatsu and Wurtz 1988; Newsome et al. 1988). MST also carries eye and head velocity signals (3rd criterion) (Thier and Erickson 1992) and is modulated by eye (Bremmer et al. 1997; Erickson and Thier 1991; Komatsu and Wurtz 1988; Squatrito and Maioli 1997; Thier and Erickson 1992) and head position (Bremmer et al. 1997) in a gain-like fashion (1st criterion) (Andersen et al. 1990; Squatrito and Maioli 1997), a major requirement for reference frame transformations (Andersen 1997). These latter eye and head position signals could also be used to estimate torsion using an internal model of 3D eye movements (2nd criterion, see DISCUSSION in the preceding text). A straightforward testable prediction of this hypothesis is that MST receptive fields and tuning curves should be modulated by ocular torsion.

Implications

This study has many implications for studies using smooth pursuit or other visually guided actions to moving targets. Importantly, the brain always needs to perform a visuomotor velocity transformation. Therefore extraretinal signals might unexpectedly influence the outcome of an experiment. This is not only true for all vision and visuomotor studies on healthy subjects or primates but might be more important when considering brain-damaged patients with deficits in areas required for visuomotor velocity conversion. Therefore errors can only be interpreted appropriately when this transformation is considered.

Moreover, the visuomotor velocity transformation is not limited to smooth pursuit eye movements. The perception of movement direction must perform some sort of transformation, depending on the reference frame used by the perceptual measure (e.g., space- or head-centered). It is also unknown whether and how other eye movement systems that rely on retinal motion signals deal with the geometry required for the sensory input. For example, anticipatory smooth pursuit would have to recall a stored velocity memory in a spatially accurate fashion across different 3D eye positions. To be spatially accurate, optokinetic stimuli would need to be transformed into accurate smooth ocular following responses. Because the optokinetic response is generated by different neural pathways (Ilg 1997), this would suggest that the optokinetic system accounts for the 3D geometry of the eyes.

Although the mathematics of the velocity transformation is probably the simplest in the eye movement system, other motor systems such as the head or arm (for reaching), also need to perform velocity transformations that might include other factors, e.g., head orientation. However, these transformations are beyond the scope of this paper and will be considered in future studies. Furthermore, all of these transformations include the situation of self-motion; our eyes, head, or whole body might move while we track a target, reach out for an object, or catch a ball. This suggests that, in general, signals about self-induced motion must be integrated in the equations underlying the visuomotor velocity transformation for perception and action.

APPENDIX

We used a model of 3D eye position and simulated different hypotheses for the visuomotor velocity transformation, according to Listing's law. We also incorporated static and dynamic VOR to account for ocular counter-roll with different gains. Retinal geometry was modeled using spherical projections (see also Blohm and Crawford 2007). Using quaternion algebra, eye-in-head rotation can be described by the following quaternion q (Tweed 1997a)

$$q = q_L q_{PP} \tag{A1}$$

$$\text{with } q_L = \sqrt{-\begin{bmatrix} 0 \\ \vec{e} \end{bmatrix} q_{LP}} \tag{A2}$$

$$\text{and } q_{PP} = \sqrt{q_{LP}^{-1}[0010]^T} \tag{A3}$$

q_L is the Listing's law quaternion and q_{PP} is the quaternion describing the primary position of the eyes in the orbit. Quaternions can be viewed as operators describing a rotation of angle θ around the rotation axis $\bar{r}$ such that $q = [\cos\theta/2 \ \bar{r}\cdot\sin\ \theta/2]^T$ and the components of the rotation axis describe vertical, torsional and horizontal eye rotations, respectively. $\vec{e}$ is the normalized vector of current eye-in-head direction (i.e., the vector describing the viewing direction in 3D space) under which a visual stimulus was viewed. q_{LP} describes the gravity tilt of Listing's plane (part of the static vestibuloocular reflex, VOR) (Bockisch and Haslwanter 2001; Haslwanter et al. 1992).

$$q_{LP} = \begin{bmatrix} 0 \\ 0 \\ \cos\alpha \\ -\sin\alpha \end{bmatrix}, \text{ with } \alpha = \alpha_0 + g_P \cdot \alpha_P \tag{A4}$$

In an idealized form of Listing's law, this gravity tilt is zero ($\alpha_0 = 0°$), such that the reference position for eye rotations is the exact straight-ahead vector. An idealized Listing's law produces zero torsion at all eye positions (given the head is upright). For the simulations performed here, we used a default tilt angle for Listing's plane in the head upright position that was $\alpha_0 = 5°$. When the head moves around the inter-aural axis (head pitch movement) about an angle α_P, the Listing's plane pitches with an average gain of $g_P = 0.05$ (Bockisch and Haslwanter 2001; Haslwanter et al. 1992). In addition to the pitch component of the rotational static VOR, we also implemented the ocular counter-roll for both the static and dynamic conditions

$$q_{OCR} = \begin{bmatrix} \cos\beta \\ 0 \\ \sin\beta \\ 0 \end{bmatrix}, \text{ with } \beta = g_{R,S} \cdot \beta_R + g_{R,D}(f) \cdot \beta_R \tag{A5}$$

The counter-roll angle β depended on the head roll angle β_R and was composed of a static VOR component (gain, $g_{R,S}$) and a frequency-dependent (f) dynamic VOR component (gain, $g_{R,D}$). From *Eq. A5*, one can immediately see that the required compensation for ocular counter-roll (Fig. 8) is linear with static head roll β_R.

The total quaternion description of eye-in-head position was then $Q = qq_{OCR}$ and a position p in retinal coordinates was transformed into head-centered coordinates p' using quaternion rotation, i.e.

$$p' = \overline{Q}pQ \quad \text{(A6)}$$

where $\bar{Q}$ is the quaternion conjugate (see Blohm and Crawford 2007 or Kuipers 2002 for a summary of quaternion algebra). This was mainly used to determine the rotation of the projected spatial cardinal axes onto the retina (Fig. 5). For example, take an idealized Listing's law ($\alpha = 0$) leading to the identity quaternion for q_{PP} (*Eq. A3*) and a roughly 45° oblique up-right fixation position. This results in $\vec{e} = (1/2\ 1/\sqrt{2}\ 1/2)^T$ and (using *Eqs. A2* and *A4*) $q_L = \sqrt{-(0\ \frac{T}{\vec{e}})^T(0\ 0\ 1\ 0)^T} = (0.92\ 0.27\ 0\ -0.27)^T$. q_L is then the eye position quaternion because multiplication with the identity quaternion (*Eq. A1*) keeps q_L unchanged. Applying *Eq. A6* using a purely vertical retinal target position such as $p = (0\ 0\ 0\ 1)^T$ results in $p' = (0\ -0.15\ -0.5\ 0.85)^T$. The latter describes the retinal vertical vector p projected into a head-centered coordinate frame, where the last three values are the *x, y,* and *z* positions in head-centered coordinates. Two things are worth mentioning here. *1*) The *y* component (coding distance) is nonzero because of the rotation of a 3D vector. Because the retina only codes 2D positions and we consider targets on a flat fronto-parallel screen, this depth component is not of interest to us. *2*) The x-component is nonzero. This reflects the rotation of the retinal vertical axis with respect to the head-centered (or spatial) vertical, the phenomenon we are interested in. Straight-forward computations lead to an approximate angular rotation of −10°, i.e., for up-right fixations, the head-centered representation is rotated clockwise with respect to the retinal image (see Fig. 5). The difference in rotation amplitude between our example here and the predictions from Fig. 5 result from $\alpha \neq 0$.

ACKNOWLEDGMENTS

The authors thank Dr. A. Z. Khan for helpful comments on the manuscript and the subjects for kind participation. The scientific responsibility rests with its authors.

GRANTS

This paper presents research results of the Belgian Network DYSCO (Dynamical Systems, Control, and Optimization) funded by the Interuniversity Attraction Poles Programme, initiated by the Belgian State, Science Policy Office. G. Blohm held a Marie Curie fellowship within the 6th Framework Program (EU) and was supported by Fonds National de la Recherche Scientifique (FNRS), the Botterell Foundation, the Canadian Foundation for Innovation, the Ontario Research Foundation and National Sciences and Engineering Research Council. P. Lefevre was supported by the FNRS, the Fondation pour la Recherche Scientifique Médicale, Actions de Recherche Concertées, the Fonds Spéciaux de Recherche of the Université catholique de Louvain, the European Space Agency, and Prodex Grant C90232 from Belgian Science Policy.

DISCLOSURES

No conflicts of interest, financial or otherwise, are declared by the author(s).

REFERENCES

Adeyemo B, Angelaki DE. Similar kinematic properties for ocular following and smooth pursuit eye movements. *J Neurophysiol* 93: 1710–1717, 2005.

Andersen RA. Multimodal integration for the representation of space in the posterior parietal cortex. *Philos Trans R Soc Lond B Biol Sci* 352: 1421–1428, 1997.

Andersen RA, Asanuma C, Essick G, Siegel RM. Corticocortical connections of anatomically and physiologically defined subdivisions within the inferior parietal lobule. *J Comp Neurol* 296: 65–113, 1990.

Angelaki DE, Hess BJ. Control of eye orientation: where does the brain's role end and the muscle's begin? *Eur J Neurosci* 19: 1–10, 2004.

Badler JB, Heinen SJ. Anticipatory movement timing using prediction and external cues. *J Neurosci* 26: 4519–4525, 2006.

Banks MS, Hooge IT, Backus BT. Perceiving slant about a horizontal axis from stereopsis. *J Vision* 1: 55–79, 2001.

Battaglia-Mayer A, Caminiti R, Lacquaniti F, Zago M. Multiple levels of representation of reaching in the parieto-frontal network. *Cereb Cortex* 13: 1009–1022, 2003.

Blohm G, Crawford JD. Computations for geometrically accurate visually guided reaching in 3-D space. *J Vision* 7: 1–22, 2007.

Blohm G, Khan AZ, Crawford JD. Spatial transformations for eye-head coordination. In: *Encyclopedia of Neuroscience*, edited by Squire LR. Oxford: Elsevier, 2009, p. 203–211.

Blohm G, Khan AZ, Ren L, Schreiber KM, Crawford JD. Depth estimation from retinal disparity requires eye and head orientation signals. *J Vision* 8: 31–23, 2008b.

Blohm G, Missal M, Lefevre P. Interaction between smooth anticipation and saccades during ocular orientation in darkness. *J Neurophysiol* 89: 1423–1433, 2003.

Bockisch CJ, Haslwanter T. Three-dimensional eye position during static roll and pitch in humans. *Vision Res* 41: 2127–2137, 2001.

Bockisch CJ, Straumann D, Haslwanter T. Eye movements during multi-axis whole-body rotations. *J Neurophysiol* 89: 355–366, 2003.

Bremmer F, Ilg UJ, Thiele A, Distler C, Hoffmann KP. Eye position effects in monkey cortex. I. Visual and pursuit-related activity in extrastriate areas MT and MST. *J Neurophysiol* 77: 944–961, 1997.

Bruno P, Van den Berg AV. Torsion during saccades between tertiary positions. *Exp Brain Res* 117: 251–265, 1997.

Carl JR, Gellman RS. Human smooth pursuit: stimulus-dependent responses. *J Neurophysiol* 57: 1446–1463, 1987.

Celebrini S, Newsome WT. Neuronal and psychophysical sensitivity to motion signals in extrastriate area MST of the macaque monkey. *J Neurosci* 14: 4109–4124, 1994.

Chowdhury SA, Takahashi K, DeAngelis GC, Angelaki DE. Does the middle temporal area carry vestibular signals related to self-motion? *J Neurosci* 29: 12020–12030, 2009.

Chukoskie L, Movshon JA. Modulation of visual signals in macaque MT and MST neurons during pursuit eye movement. *J Neurophysiol* 102: 3225–3233, 2009.

Churchland AK, Lisberger SG. Discharge properties of MST neurons that project to the frontal pursuit area in macaque monkeys. *J Neurophysiol* 94: 1084–1090, 2005.

Crawford JD, Guitton D. Visual-motor transformations required for accurate and kinematically correct saccades. *J Neurophysiol* 78: 1447–1467, 1997.

Crawford JD, Martinez-Trujillo JC, Klier EM. Neural control of three-dimensional eye and head movements. *Curr Opin Neurobiol* 13: 655–662, 2003.

Crawford JD, Medendorp WP, Marotta JJ. Spatial transformations for eye-hand coordination. *J Neurophysiol* 92: 10–19, 2004.

Crawford JD, Vilis T. Axes of eye rotation and Listing's law during rotations of the head. *J Neurophysiol* 65: 407–423, 1991.

de Brouwer S, Missal M, Barnes G, Lefevre P. Quantitative analysis of catch-up saccades during sustained pursuit. *J Neurophysiol* 87: 1772–1780, 2002.

de Brouwer S, Missal M, Lefevre P. Role of retinal slip in the prediction of target motion during smooth and saccadic pursuit. *J Neurophysiol* 86: 550–558, 2001.

Demer JL. Pivotal role of orbital connective tissues in binocular alignment and strabismus: the Friedenwald lecture. *Invest Ophthalmol Vis Sci* 45: 729–738; 728, 2004.

Demer JL. Current concepts of mechanical and neural factors in ocular motility. *Curr Opin Neurol* 19: 4–13, 2006.

Demer JL. Mechanics of the orbita. *Dev Ophthalmol* 40: 132–157, 2007.

Deneve S, Latham PE, Pouget A. Efficient computation and cue integration with noisy population codes. *Nat Neurosci* 4: 826–831, 2001.

Dicke PW, Thier P. The role of cortical area MST in a model of combined smooth eye-head pursuit. *Biol Cybern* 80: 71–84, 1999.

Dimitrova DM, Shall MS, Goldberg SJ. Stimulation-evoked eye movements with and without the lateral rectus muscle pulley. *J Neurophysiol* 90: 3809–3815, 2003.

Dursteler MR, Wurtz RH. Pursuit and optokinetic deficits following chemical lesions of cortical areas MT and MST. *J Neurophysiol* 60: 940–965, 1988.

Erickson RG, Thier P. A neuronal correlate of spatial stability during periods of self-induced visual motion. *Exp Brain Res* 86: 608–616, 1991.

Fetter M, Misslisch H, Sievering D, Tweed D. Effects of full-field visual input on the three-dimensional properties of the human vestibuloocular reflex. *J Vestib Res* 5: 201–209, 1995.

Ghasia FF, Meng H, Angelaki DE. Neural correlates of forward and inverse models for eye movements: evidence from three-dimensional kinematics. *J Neurosci* 28: 5082–5087, 2008.

Harris L, Beykirch K, Fetter M. The visual consequences of deviations in the orientation of the axis of rotation of the human vestibulo-ocular reflex. *Vision Res* 41: 3271–3281, 2001.

Haslwanter T, Straumann D, Hess BJ, Henn V. Static roll and pitch in the monkey: shift and rotation of Listing's plane. *Vision Res* 32: 1341–1348, 1992.

Hepp K, Van Opstal AJ, Straumann D, Hess BJ, Henn V. Monkey superior colliculus represents rapid eye movements in a two-dimensional motor map. *J Neurophysiol* 69: 965–979, 1993.

Ilg UJ. The role of areas MT and MST in coding of visual motion underlying the execution of smooth pursuit. *Vision Res* 48: 2062–2069, 2008.

Ilg UJ. Slow eye movements. *Prog Neurobiol* 53: 293–329, 1997.

Ilg UJ, Schumann S, Thier P. Posterior parietal cortex neurons encode target motion in world-centered coordinates. *Neuron* 43: 145–151, 2004.

Ilg UJ, Thier P. The neural basis of smooth pursuit eye movements in the rhesus monkey brain. *Brain Cogn* 68: 229–240, 2008.

Inaba N, Shinomoto S, Yamane S, Takemura A, Kawano K. MST neurons code for visual motion in space independent of pursuit eye movements. *J Neurophysiol* 97: 3473–3483, 2007.

Klier EM, Meng H, Angelaki DE. Three-dimensional kinematics at the level of the oculomotor plant. *J Neurosci* 26: 2732–2737, 2006.

Komatsu H, Wurtz RH. Relation of cortical areas MT and MST to pursuit eye movements. I. Localization and visual properties of neurons. *J Neurophysiol* 60: 580–603, 1988.

Krauzlis RJ. Recasting the smooth pursuit eye movement system. *J Neurophysiol* 91: 591–603, 2004.

Krauzlis RJ, Lisberger SG. A control systems model of smooth pursuit eye movements with realistic emergent properties. *Neural Comput* 1: 116–122, 1989.

Krauzlis RJ, Miles FA. Release of fixation for pursuit and saccades in humans: evidence for shared inputs acting on different neural substrates. *J Neurophysiol* 76: 2822–2833, 1996.

Kuipers JB. *Quaternions and Rotation Sequences: A Primer with Applications to Orbits, Aerospace and Virtual Reality*. Princeton, NJ: Princeton University Press, 2002.

Lisberger SG. Visual guidance of smooth-pursuit eye movements: sensation, action, and what happens in between. *Neuron* 66: 477–491, 2010.

Lisberger SG, Morris EJ, Tychsen L. Visual motion processing and sensory-motor integration for smooth pursuit eye movements. *Annu Rev Neurosci* 10: 97–129, 1987.

McClung JR, Allman BL, Dimitrova DM, Goldberg SJ. Extraocular connective tissues: a role in human eye movements? *Invest Ophthalmol Vis Sci* 47: 202–205, 2006.

Misslisch H, Hess BJ. Three-dimensional vestibuloocular reflex of the monkey: optimal retinal image stabilization versus listing's law. *J Neurophysiol* 83: 3264–3276, 2000.

Mok D, Ro A, Cadera W, Crawford JD, Vilis T. Rotation of Listing's plane during vergence. *Vision Res* 32: 2055–2064, 1992.

Moore ST, Haslwanter T, Curthoys IS, Smith ST. A geometric basis for measurement of three-dimensional eye position using image processing. *Vision Res* 36: 445–459, 1996.

Newsome WT, Wurtz RH, Komatsu H. Relation of cortical areas MT and MST to pursuit eye movements. II. Differentiation of retinal from extraretinal inputs. *J Neurophysiol* 60: 604–620, 1988.

Optican LM. Sensorimotor transformation for visually guided saccades. *Ann NY Acad Sci* 1039: 132–148, 2005.

Pack C, Grossberg S, Mingolla E. A neural model of smooth pursuit control and motion perception by cortical area MST. *J Cogn Neurosci* 13: 102–120, 2001.

Peterka RJ, Merfeld DM. Calibration techniques for video-oculography (Abstract). *J Vestibul Res* 6: 75, 1996.

Quaia C, Optican LM. Commutative saccadic generator is sufficient to control a 3-D ocular plant with pulleys. *J Neurophysiol* 79: 3197–3215, 1998.

Robinson DA. The mechanics of human smooth pursuit eye movement. *J Physiol* 180: 569–591, 1965.

Schreiber KM, Crawford JD, Fetter M, Tweed D. The motor side of depth vision. *Nature* 410: 819–822, 2001.

Schreiber K, Haslwanter T. Improving calibration of 3-D video oculography systems. *IEEE Trans Biomed Eng* 51: 676–679, 2004.

Snyder LH. Coordinate transformations for eye and arm movements in the brain. *Curr Opin Neurobiol* 10: 747–754, 2000.

Sparks DL, Mays LE. Signal transformations required for the generation of saccadic eye movements. *Annu Rev Neurosci* 13: 309–336, 1990.

Squatrito S, Maioli MG. Encoding of smooth pursuit direction and eye position by neurons of area MSTd of macaque monkey. *J Neurosci* 17: 3847–3860, 1997.

Thier P, Erickson RG. Responses of visual-tracking neurons from cortical area MST-I to visual, eye and head motion. *Eur J Neurosci* 4: 539–553, 1992.

Tian JR, Crane BT, Ishiyama A, Demer JL. Three dimensional kinematics of rapid compensatory eye movements in humans with unilateral vestibular deafferentation. *Exp Brain Res* 182: 143–155, 2007.

Tweed D. Three-dimensional model of the human eye-head saccadic system. *J Neurophysiol* 77: 654–666, 1997a.

Tweed D. Visual-motor optimization in binocular control. *Vision Res* 37: 1939–1951, 1997b.

Tweed D, Fetter M, Andreadaki S, Koenig E, Dichgans J. Three-dimensional properties of human pursuit eye movements. *Vision Res* 32: 1225–1238, 1992.

Tweed D, Vilis T. Geometric relations of eye position and velocity vectors during saccades. *Vision Res* 30: 111–127, 1990.

Tweed D, Vilis T. Implications of rotational kinematics for the oculomotor system in three dimensions. *J Neurophysiol* 58: 832–849, 1987.

van Ee R, van Dam LC. The influence of cyclovergence on unconstrained stereoscopic matching. *Vision Res* 43: 307–319, 2003.

Van Rijn LJ, Van den Berg AV. Binocular eye orientation during fixations: Listing's law extended to include eye vergence. *Vision Res* 33: 691–708, 1993.

Wertheim AH. On the relativity of perceived motion. *Acta Psychol* 48: 97–110, 1981.